Journal of Earth Science, *Vol. 22*, *No. 2*, *p. 176–181*, *April 2011* *ISSN 1674-487X*
Printed in China
DOI: 10.1007/s12583-011-0170-0

Parallel Numerical Analysis on the Rheology of the Martian Ice-Rock Mixture

Jing Huimin (景惠敏), **Zhang Huai** (张怀), **Li Han** (李菡)
Laboratory of Computational Geodynamics, *Graduate University of Chinese Academy of Sciences*, *Beijing* 100049, *China*
David A Yuen
Department of Geology and Geophysics and Minnesota Supercomputing Institute, *University of Minnesota*, *Minneapolis*, *MN* 55415, *USA*
Shi Yaolin* (石耀霖)
Laboratory of Computational Geodynamics, *Graduate University of Chinese Academy of Sciences*, *Beijing* 100049, *China*

ABSTRACT: The distribution and amount of ground ice on Mars is an important issue to be addressed for the future exploration of the planet. The occurrence of interstitial ice in Martian frozen ground is indicated by landforms, such as fluidized ejecta craters, softened terrain, and fretted channels. However, experimental data on the rheology of ice-rock mixture under Martian physical conditions are sparse, and the amount of ground ice that is required to produce the viscous deformation observed in Martian ice-related landforms is still unknown. In our study, we put forward a three-dimensional non-Newtonian viscous finite element model to investigate the behavior of ice-rock mixtures numerically. The randomly distributed tetrahedral elements are generated in regular domain to represent the natural distribution of ice-rock materials. Numerical simulation results show that when the volume of rock is less than 40%, the rheology of the mixture is dominated by ice, and there is occurrence of a brittle-ductile transition when ice fraction reaches a certain value. Our preliminary results contribute to the knowledge of the determination of the rheology and ice content in Martian ice-rock mixture. The presented model can also be utilized to evaluate the amount of ground ice on Mars.

KEY WORDS: parallel simulation, rheology, ice-rock mixture, Mars.

INTRODUCTION

The physical state of water on Mars has fundamental ramifications for both climatology and astrobiology (Aharonson and Schorghofer, 2006; Whalley and Azizi, 2003). Subsurface radar sounding data indicate that lobate debris aprons found in Deuteronilus Mensae in the mid-northern latitudes of Mars are composed predominantly of the mixture of rock debris and water ice (Plaut et al., 2009). The occurrence of interstitial ice in Martian frozen ground is indicated by landforms, such as fluidized ejecta craters, softened

This study was supported by the National Basic Research Program of China (No. 2008CB425701), the National Natural Science Foundation of China (No. 40774049), the National Science and Technology Project (No. SinoProbe-07), Institute of Earthquake Science, China Earthquake Administration, and Senior Visiting Professorship of Chinese Academy of Sciences and CMG Program of the U.S. National Science Foundation.
*Corresponding author: shiyl@gucas.ac.cn

Manuscript received September 22, 2010.
Manuscript accepted November 16, 2010.

terrain, or fretted channels (Byrne et al., 2009; Milliken et al., 2003). Some of these features, like lobate debris aprons, are theorized to have been formed by the viscous deformation of ice-rock mixture like rock glaciers on earth (Li et al., 2005). The rheology of ice-rock mixtures has been studied under terrestrial conditions for engineering purposes at low pressure and stress near melting point (Yasui and Arakawa, 2008; Mangold, 2003). However, experimental data on the rheology of ice-rock mixture under Martian physical conditions are sparse, and the amount of ground ice that is needed to produce the viscous deformation observed in Martian ice-related landforms is still under investigation (Durham et al., 2009). Furthermore, it is time-consuming and also very expensive to perform these kinds of measurements in the laboratory. Thus, numerical simulation is a practical solution.

Our study investigates the behavior of ice-rock mixtures numerically. The large-scale three-dimensional finite element tests are proposed in order to determine the rheology of the Martian ice-rock mixture. The randomly distributed tetrahedral elements are generated to represent the natural ice-rock mixtures. This method has been successfully applied to investigating the rheology of rocks composed of multiple minerals (Cui et al., 2008). The randomly generated tetrahedral elements are partitioned to denote the rock or the ice material, respectively. Each subpartition can be assigned different parameters of ice or rock components. Then, the stress and strain rates of the ice-rock mixture under the physical conditions similar to Martian subsurface are produced by finite element numerical tests. For a given component ratio, a cluster of numerical models are generated randomly and analyzed statistically.

Our numerical test results are largely in accordance with the experimental results under terrestrial conditions, which can verify the rheological parameters of the ice-rock mixture on Mars. The randomly distributed ice-rock mixture shows the occurrence of a brittle-ductile transition when ice fraction at a certain proportion. However, the difference still exists due to difference between the realistic and the numerically generated distribution of ice or rock components. In order to reduce the measurement error to a reasonable range, the numerical specimen must be large enough to include sufficient number of particles (tetrahedral elements or their subpartitions).

NUMERICAL MODEL CONFIGURATION

Governing Equations

The steady-state viscous strain rate $\dot{\varepsilon} = (\mathrm{d}\varepsilon / \mathrm{d}t)_{ss}$ of polycrystalline ice is described by a power law relationship (Weertman, 1983)

$$\dot{\varepsilon} = A\sigma^n \exp(-E/RT) \tag{1}$$

where σ is the differential stress; T is the temperature; R is the gas constant; and A, n, and E are parameters characterizing the material, respectively, A denotes the constant of the viscous parameter, and it can be the function of temperature and bulk pressure, E represents the activation energy. When the temperature is constant, equation (1) can be expressed by

$$\dot{\varepsilon} = B\sigma^n \tag{2}$$

where B is the constant, and B=Aexp(-E/RT) is the inverse of the effective viscosity.

The equations of equilibrium, geometric, effective stress, effective strain, and constitutive could be respectively expressed as

$$\sigma_{ij,j} + f_i = 0 \tag{3}$$

$$\dot{\varepsilon}_{ij} = (u_{i,j} + u_{j,i})/2 \tag{4}$$

$$\bar{\sigma} = \sqrt{\frac{3}{2}[\sigma_{xx}{}^2 + \sigma_{yy}{}^2 + \sigma_{zz}{}^2 + \frac{1}{2}(\sigma_{xy}{}^2 + \sigma_{yz}{}^2 + \sigma_{xz}{}^2)]} \tag{5}$$

$$\bar{\dot{\varepsilon}} = \sqrt{\frac{2}{3}[\varepsilon_{xx}{}^2 + \varepsilon_{yy}{}^2 + \varepsilon_{zz}{}^2 + \frac{1}{2}(\varepsilon_{xy}{}^2 + \varepsilon_{yz}{}^2 + \varepsilon_{xz}{}^2)]} \tag{6}$$

$$\bar{\sigma} = \eta \bar{\dot{\varepsilon}}^{-\frac{1}{n}} \tag{7}$$

we can get the average value of effective viscosity η by least square method as

$$\lg \eta = \frac{1}{N}\sum_{i=1}^{N}(\lg \bar{\sigma}_i - \frac{1}{n}\lg \bar{\dot{\varepsilon}}_i) \tag{8}$$

where the subscript i indicates the tetrahedral elements; and N is the total number of elements in our numerical model.

Finite Element Model

Our numerical specimen is a cylinder containing a mixture of randomly distributed sand and ice grains, as shown in Fig. 1. The cylinder measures 10 mm in diameter and 40 mm in length. Conventional triaxial compression tests are conducted to calculate the instantaneous strain rate by large-scale parallel finite element simulations. The hydrostatic pressure is fixed to 12 MPa. It is consistent with the pressure in Martian subsurface at 1 km in depth. The constant temperature T=263 K is considered. B and n are constants for ice and rock. The parameters utilized in our study are listed in Table 1. In our numerical tests, η= 1.091 0×10^8 and n=3, respectively.

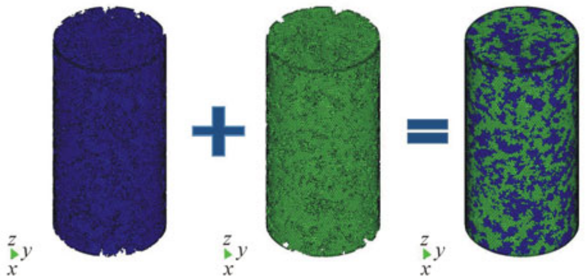

Figure 1. The randomly distributed spatial granularity specimen consisted of ice and rock. It displays our finite element numerical model created by randomly mixed ice and rock. The left figure shows the ice and rock's spatial distribution, and each color represents one kind of component. The right figure shows the randomly distributed spatial configurations of ice and rock.

Table 1 Parameters in ice-rock mixture numerical simulation (Turcotte and Schubert, 2002)

Parameters	Symbol	Value
Temperature (K)	T	263
Gas constant (J·mol^{-1}·K^{-1})	R	8.314
A for ice (MPa^{-n}·s^{-1})	A_{ice}	8.8×10^5
n for ice	n_{ice}	3
E for ice (kJ/mol)	E_{ice}	60.7
A for rock (MPa^{-n}·s^{-1})	A_{rock}	6.7×10^{-12}
n for rock	n_{rock}	6.5
E for rock (kJ/mol)	E_{rock}	268

Parallel Computation

Previous work indicates that to reduce the measurement error in the simulation of rheology, the numerical specimen must be large enough to include sufficient number of particles (Banks et al., 2008). Thus, large-scale parallel finite element simulation has to be used. In our study, the model has been divided into 28 698 grids, which formed 1 035 297 tetrahedrons. Since one grid denotes one grain of ice or rock, these grids can represent grains of very small sizes. In our parallel solver, we adopted the domain decomposition method (DDM) (Craig, 1997) to divide the computing domain into sub-domains. The preconditioned Krylov-subspace parallel solvers are utilized on distributed computer node to calculate linear sparse system simultaneously. Figure 2 illustrates the partitioned subdomains and the dual points on the inner boundaries of one subdomain.

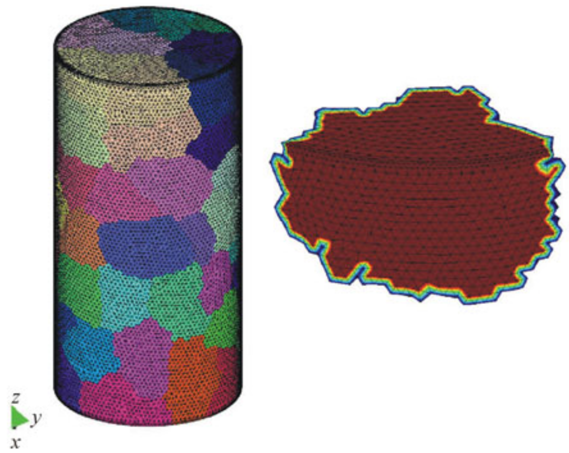

Figure 2. Partitioned subdomains in DDM parallel solver (left) and the dual point (grids with different colors) in one subdomain (right).

RESULTS AND DISCUSSION

We calculated the strain, stress, the effective stress, the effective strain rate, and the effective rheology by equations (5)–(8). To verify our parallel numerical model, we first calculated the pure ice model. The input parameters are listed in Table 1. The results of the differential stress and strain are shown in Fig. 3. The parameters calculated from the results are η=1.098 1×10^8 and n=3.007. Compared with input parameters (η=1.091 0×10^8 and n=3), the relative errors are 0.65% and 0.23%.

After we verified the feasibility of pour ice model, we use the same code to conduct the ice-rock mixture simulation. We supposed that the rock is quartz, whose parameters were listed in Table 1. To compare our numerical test results with the experimental data, we set the volume fraction of ice in the mixture to be 48%, which is the same with the experiment made by

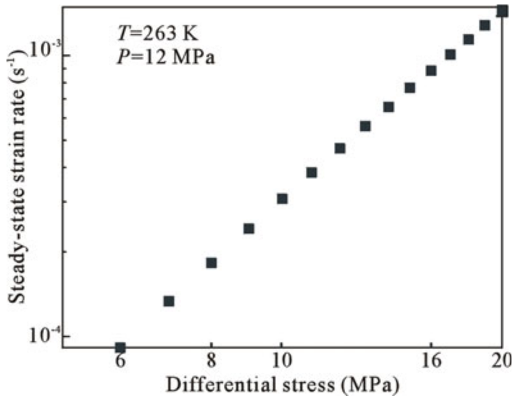

Figure 3. Steady-state strain rate versus differential stress for ice model.

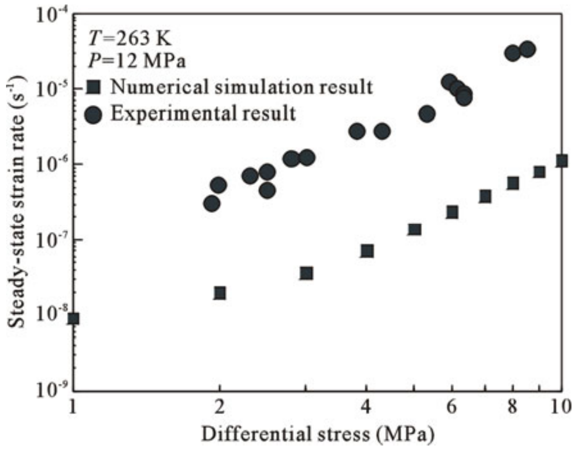

Figure 4. Steady-state strain rate versus differential stress for comparison at a fixed ice fraction of 48% with fixed temperature and pressure. Our numerical simulation results are compared with the experimental results (Mangold, 2003).

Mangold (2003). Figure 4 shows the comparison of our numerical simulation results and experimental results. This comparison proved the feasibility and efficiency of our method.

In Fig. 4, we can also see that there are different magnitudes of simulation results and experimental results. As mentioned before, since the experiments at very low temperature and high pressure are time-consuming and expensive to perform, there are no accurate parameters available at the present time. The parameters used in our study are extrapolated from empirical formulas in stead of real experiments, which possibly introduces the differences. Another reason is that we did not consider the effects of dispersed particulates. Some experimental results suggest that viscous drag occurs in the ice as it flows around the hard particulates, and mixed-phase ice is tougher than the pure ice (Song et al., 2007; Durhan et al., 1992).

Under different volume fractions of ice and rock, we generated a cluster of numerical models. The strain, stress, the effective stress, the effective strain rate, and the effective rheology were also calculated and analyzed statistically. Figure 5 shows that the effective rheology of the mixture varies with the volume fraction of rock, which changes from 0 to 1. The rheology parameters of the mixture are gradually increased from the rheology of ice to that of the rock. When the volume of rock is less than 40%, the rheology of the mixture is dominated by ice. There is occurrence of a brittle-ductile transition when ice fractions at a certain value. However, the values of rheology are different even under a certain component ratio due to the distribution of components. As components are randomly distributed in our numerical model, the error decreased with the increasing of the ratio between the volume of the specimen and average volume of gains. In order to confine the error to a reasonable range, the ratio value is set to be 2.0×10^4 in this study. Because we generate new randomly distributed models each time, the spatial arrangement of grains would change the rheology of the mixture. However, at a constant volume fraction, there are many other factors that would induce the difference of rheology values, e.g., randomize, micro fracture, and pore shape. How these factors influence the mixture needs further study in order to better understand the porosity and ice content of ice-rock mixture on Martin surface. We will do these researches in the future.

CONCLUSIONS

Our numerical benchmark showed that utilizing large-scale parallel finite element numerical simulation method to investigate the rheology of ice-rock mixture is effective and feasible. If we know the rheology parameters of the components under certain conditions, we can calculate the parameters of the mixtures by numerical experiments and statistical analysis rather than the time-consuming and expensive laboratorial experiments. Since parallel computing is much more convenient and efficient than the

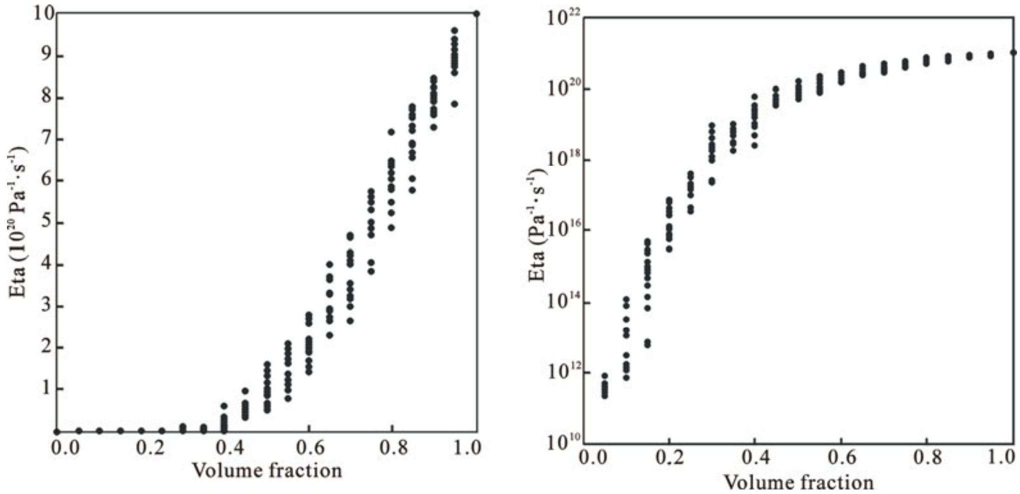

Figure 5. Effective rheology of the mixture varies with the volume fraction of rock that changes from 0 to 1.

Table 2 Difference between the simulation (our study) and the experimental results (Mangold, 2003)

Simulation results (our study)		Experimental results (Mangold, 2003)	
Differential stress (MPa)	Steady-state strain rate (s^{-1})	Differential stress (MPa)	Steady-state strain rate (s^{-1})
1.0	$0.868\,7\times10^{-8}$	1.92	3.145×10^{-7}
2.0	$0.190\,4\times10^{-7}$	1.98	5.391×10^{-7}
3.0	$0.351\,6\times10^{-7}$	2.29	7.552×10^{-7}
4.0	$0.693\,7\times10^{-7}$	2.48	4.712×10^{-7}
5.0	$0.133\,4\times10^{-6}$		8.355×10^{-7}
6.0	$0.234\,1\times10^{-6}$	2.80	1.252×10^{-6}
7.0	$0.376\,4\times10^{-6}$	3.01	1.295×10^{-6}
8.0	$0.564\,8\times10^{-6}$	3.80	2.907×10^{-6}
9.0	$0.806\,0\times10^{-6}$	4.28	2.907×10^{-6}
10.0	$0.110\,7\times10^{-5}$	5.29	4.819×10^{-6}
——	——	5.88	1.280×10^{-5}
——	——	6.08	1.046×10^{-5}
——	——	6.28	9.141×10^{-6}
——	——		7.723×10^{-6}
——	——	7.93	3.075×10^{-5}
——	——	8.53	3.402×10^{-5}

laboratorial experiment, by changing the volume fraction and differential pressure conditions, we can establish a direct relationship of rheology parameter of one mixture consisting of any kind of components. These results will contribute to the knowledge of the porosity and ice content of Martian ice-rock mixture. It also can be used to estimate the amount of ground ice in different latitudes on Mars. The estimated parameters can also be utilized to uncover the strength profiles of the Martian megaregolith and geomorphic consequences.

ACKNOWLEDGMENTS

This work was supported by the National Basic Research Program of China (No. 2008CB425701), the National Natural Science Foundation of China (No. 40774049), and the National Science and Technology Project (No. SinoProbe-07). We thank Institute of Earthquake Science, China Earthquake Administration, who provided us with the support from the collaborative project named “Pre-study of Several Issues of Testing Ground for Numerical Forecast Earthquakes in North China”. David A Yuen was supported also by

Senior Visiting Professorship of Chinese Academy of Sciences and the CMG program of the U.S. National Science Foundation.

REFERENCES CITED

Aharonson, O., Schorghofer, N., 2006. Subsurface Ice on Mars with Rough Topography. *Journal of Geophysical Research*, 111(E11007): 1–10

Banks, M. E., McEwen, A. S., Kargel, J. S., et al., 2008. High Resolution Imaging Science Experiment (HiRISE) Observations of Glacial and Periglacial Morphologies in the Circum-Argyre Planitia Highlands, Mars. *Journal of Geophysical Research*, 113(E12015): 1–20

Byrne, S., Dundas, C. M., Kennedy, M. R., et al., 2009. Distribution of Mid-Latitude Ground Ice on Mars from New Impact Craters. *Science*, 325(5948): 1674–1676

Craig, C. D., 1997. Multigrid Methods in Science and Engineering. *IEEE Computer Society Eng*., 3: 55–68

Cui, X. J., Zhang, H., Shi, Y. L., 2008. Numerical Simulation on Rheology of Multi-mineral Rocks. *Acta Petrologica Sinica*, 24(6): 1417–1424 (in Chinese with English Abstract)

Durham, W. B., Pathare, A. V., Stern, L. A., et al., 2009. Mobility of Icy Sand Packs, with Application to Martian Permafrost. *Geophysical Research Letters*, 36(L23203): 1–5

Durham, W. B., Kirby, S. H., Stern, L. A., 1992. Effect of Dispersed Particulates on the Rheology of Water Ice at Planetary Conditions. *Journal of Geophysical Research*, 97(E12): 20883–20897

Li, H., Robinson, M. S., Jurdy, D. M., 2005. Origin of Martian Northern Hemisphere Mid-Latitude Lobate Debris Aprons. *Icarus*, 176(2): 382–394

Mangold, N., 2003. Geomorphic Analysis of Lobate Debris Aprons on Mars at Mars Orbiter Camera Scale: Evidence for Ice Sublimation Initiated by Fractures. *Journal of Geophysical Research*, 108(E4): 8021

Milliken, R. E., Mustard, J. F., Goldsby, D. J., 2003. Viscous Flow Features on the Surface of Mars: Observations from High-Resolution Mars Orbiter Camera (MOC) Images. *Journal of Geophysical Research*, 108(E6): 5057

Plaut, J. J., Safaeinili, A., Holt, R. J., et al., 2009. Radar Evidence for Ice in Lobate Debris Aprons in the Mid-Northern Latitudes of Mars. *Geophysical Research Letters*, 36: 4

Song, M., Cole, D. M., Baker, I., 2007. Effect of Fine Particles on the Flow Behavior of Polycrystalline Ice-(Ⅱ) Anelastic Behavior. *Chinese Journal of Geophysics*, 50(4): 1156–1160 (in Chinese with English Abstract)

Turcotte, D. L., Schubert, G., 2002. Geodynamics. Cambridge University Press, New York. 456

Weertman, J., 1983. Creep Deformation of Ice. *Annual Review of Earth and Planetary Sciences*, 11: 215–240

Whalley, W. B., Azizi, F., 2003. Rock Glaciers and Protalus Landforms: Analogous Forms and Ice Sources on Earth and Mars. *Journal of Geophysical Research*, 108(8032): 1–17

Yasui, M., Arakawa, M., 2008. Experimental Study on the Rate Dependent Strength of Ice-Silica Mixture with Silica Volume Fractions up to 0.63. *Geophysical Research Letters,* 35(L12206): 1–5